

# EARLY DIAGNOSIS OF ALZHEIMER'S DISEASE: A HYBRID DEEP LEARNING FRAMEWORK WITH MODIFIED CLASSIFICATION ALGORITHMS

**RAJIV K.M**

Research Scholar, Department of Computer Science and Engineering, Dr. MGR Educational and Research Institute, Chennai, Tamilnadu, India. Email: rajivkm14@gmail.com

**Dr. RAJAVARMAN V.N**

Professor, Department of Computer Science and Engineering, Dr. MGR Educational and Research Institute, Chennai, Tamilnadu, India. Email: rajavarman.vn@drmrgdu.ac.in

## Abstract

Alzheimer's disease (AD) is a gradual mental decline and incurable neurodegenerative illness that may emerge in middle or late age as a result of extensive brain degradation. Because Alzheimer's disease progresses irreversibly, early detection is critical from a clinical, social, and economic standpoint. This study product proposes a cutting-edge, simple, and early automated deep learning-based approach to predict Alzheimer's disease using a huge MRI dataset of healthy and ill people. The prediction of Alzheimer's disease using a deep learning algorithm was effectively devised and applied in this study. The performance of the Inception v3 and Hybrid CNN models was also investigated. In Alzheimer's disease prediction, a hybrid deep learning model outperforms Inception V3.

**Index Terms:** Alzheimer's disease, CNN, Inception V3, Deep learning, MRI.

## 1. INTRODUCTION

Those who suffer from Alzheimer's disease have a slow but steady loss of mental and memory abilities. Sixty percent to eighty percent of all forms of dementia are associated with Alzheimer's disease, making it a very common disorder among the elderly. Alzheimer's disease is quite common, yet there is no treatment available. There is a considerable lag time between the first symptoms of AD and the official diagnosis. Patients with mild cognitive impairment (MCI) have not yet developed Alzheimer's disease (AD), although around 30–40% of MCI patients will eventually develop AD. Brain characteristics connected with AD, such as apparent hippocampus and amygdala atrophy [1, 2] and early lateral ventricle extension, have already begun to change prior to the onset of cognitive decline in a patient with AD. Certain brain areas have begun to shrink, as shown by studies on biomarkers related with Alzheimer's disease. Therefore, it is essential to diagnose Alzheimer's disease early and accurately.

Clinical diagnosis is substantially facilitated by computer-assisted approaches, and medical image classification is a difficult task. Computed tomography [3, 4], structural MRI [5, and PET] are the most common diagnostic tools for neurodegenerative

diseases. CT scans are fast and provide high-quality images. It has the potential to be employed in the study of several diseases. However, MCI may be easily dismissed as a natural part of ageing due to the middle lobe's low resolution. PET uses transmission scanning technology to improve sensitivity and resolution, minimising the impact of tissue attenuation on the final picture. Scan the inside anatomy of a person using MRI technology, which employs magnetic resonance. The use of a rapidly varying gradient magnetic field accelerates MRI scan times, improves image clarity in soft tissues, and reduces exposure to harmful ionising radiation. The feature extraction process is crucial to the success of any image classification system. In order to do traditional research, scientists have to manually exclude AD characteristics like the hippocampus and amygdala. Frontotemporal lobe atrophy [6] is a diagnostic tool for Alzheimer's disease. Hippocampal size, as manually assessed by [7] may also be able to distinguish healthy seniors from those with moderate Alzheimer's disease. Voxel-based morphometry (VBM) was shown to be more accurate than ROI-based hippocampus volume estimate in a study by Testa et al. [8], although obtaining interaction information between voxels is difficult. Work that must be done physically introduces not just limitations but also the possibility of human error. The rapid development of AI has led to a surge of interest in using computer vision to detect Alzheimer's disease. When it comes to solving the problems that have plagued previous machine learning methods, deep learning has emerged as far and away the leader. The field of medical imaging has recently been dominated by deep learning [9, 10], which has been successfully used to automatically extract characteristics from medical images to conduct AD detection.

### 1.1 Brain Imaging Techniques for Alzheimer's disease (AD)

Brain imaging techniques [11] may be used to observe the structure, function, and pharmacology of the brains in a non-invasive manner. Imaging techniques are widely categorised as structural imaging and functional imaging [12]. Structural imaging provides information on the structure of the brain, such as neurons, synapses, glial cells, etc.

**Fig. 1. Example of structural Magnetic Resonance Imaging (MRI)**

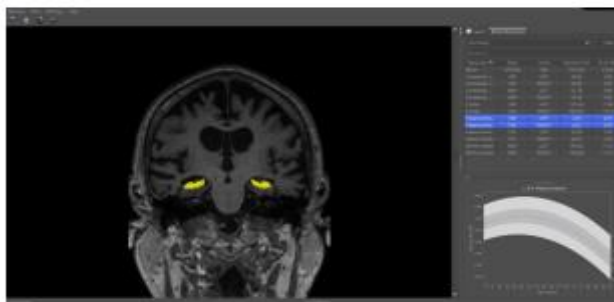
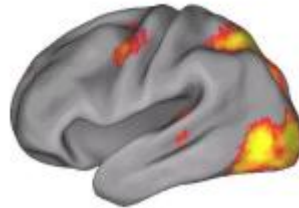


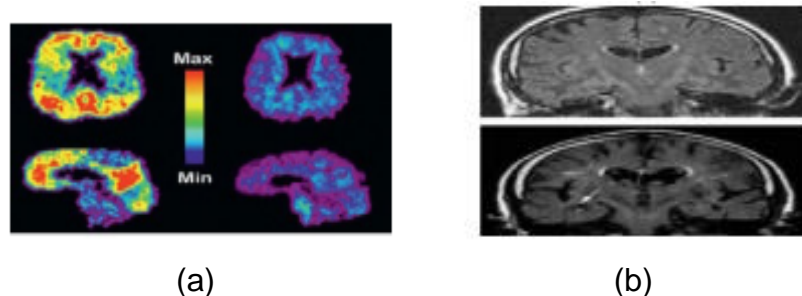
**Fig. 2. Example of functional Magnetic Resonance Imaging (fMRI)**



Functional imaging offers information on the brain's activity [13]. The following are the most often utilised neuroimaging procedures for Alzheimer's disease:

**Magnetic Resonance Image (MRI):** This imaging technology uses radio waves and magnetic fields to create high-quality 2D and 3D brain pictures. X-rays and radioactive tracers don't emit radiation. Structural MRI examines brain volumes in vivo to identify brain degeneration in Alzheimer's patients (loss of tissue, cells, neurons, etc.). Alzheimer's causes brain degeneration [14, 15]. Fig. 1 shows a brain atrophy structural MRI. fMRI is a popular approach for examining the human primary visual cortex and brain topography (Fig. 2). fMRI gives important data on brain activity and function. BOLD and ASL contrasts are sensitive to brain metabolic rate and blood flow (CBF). Figure 3a shows the brain regions of elderly people (AD patients; controls), whereas Figure 3b shows medial temporal activity. SPECT is less expensive than other modalities and sensitive for early detection of cerebral blood flow alterations [16]. This technique is still used to analyse brain activity.

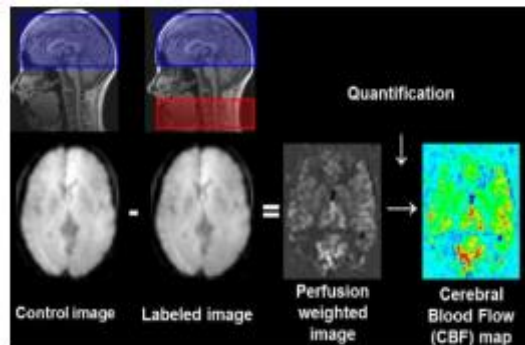
**Fig. 3: a) The brain area in older controls and AD (b) MRI scan brain in Medial Temporal atrophy.**



SPECT can accurately assess Alzheimer's patients' cerebral perfusion, according to many studies. 116 Alzheimer's sufferers were studied. 67 adults with neurological disorders, 26 without dementia, and 23 age-matched controls [17]. This research examined brain perfusion, cognitive proteins, and CSF-tau. Participants with dementia and without were separated. Cognitive functions and functional conditions were determined using the Mini-Mental State Examination, the Cambridge Cognitive Examination, and a functional grading system for symptomatic dementia. SPECT

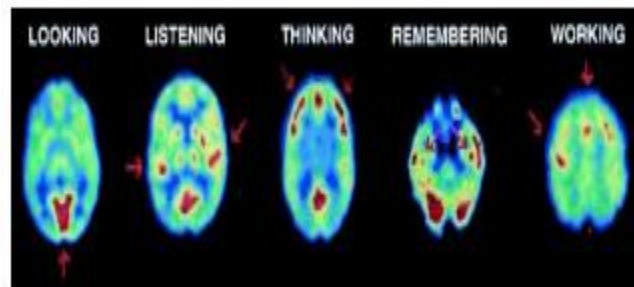
scanning associated CSF-tau protein levels. The application of precise criteria boosted the study's credibility. Prior research on bilateral parietal and temporal hypoperfusion in Alzheimer's patients found relationships between cognitive test results and SPECT findings. SPECT is better than CSF-tau protein for evaluating Alzheimer's disease, according to [18]. Fig. 4 [19] shows a 70-year-old patient's arterial spin labelling perfusion picture. The proximal arterial tree is inappropriate for our investigation due to its slow transit time.

**Fig. 4: General principle of arterial spin labelling**



**Positron Emission Tomography (PET):** In this imaging procedure, radiotracers are used, and the brain's activity is analysed as radioactive spheres. Amyloid and fluorodeoxyglucose are the two most often utilised tracers for diagnosing Alzheimer's disease, as seen in Fig. 5. Certain actions, including seeing, hearing, thinking, remembering, and working, were investigated [20], [21].

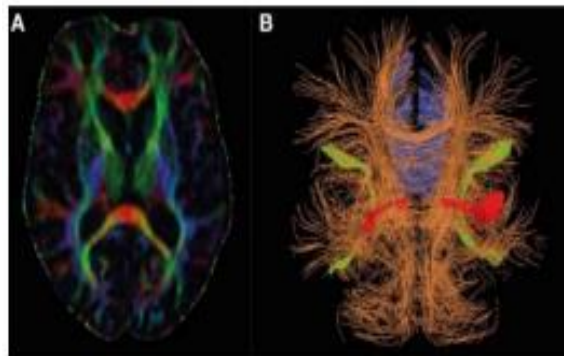
**Fig. 5: PET scan of a brain in normal condition**



Acetylcholinesterase was found using C-PMP and C-MP4A. AD patients' temporal lobes had shrunk [22]. AD-developing MCI patients saw a similar decrease. Alzheimer's and dementia patients were categorised. Participants with AD improved more than those with FTLD and PD [23]. AD PET patients had temporoparietal hypoperfusion. False-positive findings, which give little benefit to MRI, make SPECT uncomfortable for clinical usage. Neuroreceptors and FP-CIT SPECT are more helpful and easy because they allow researchers examine changes in nigrostriatal dopaminergic neurons. FP-CIT

SPECT examines water diffusion. This approach determines the brain's white matter location, orientation, and anisotropy. This method modifies water's molecular structure [24]. DTI is not a viable tool for identifying CSF biomarkers, despite extensive studies to find CSF-tau biomarkers and amyloid levels [25]. Fig. 6A shows a DTI with fractional anisotropy (red: left–right; green: anterior–posterior; blue: head–foot). Fig 6B shows DTI for AD using tractography analysis, which shows persistent AD alterations. (blue: corpus callosum; red: uncinate fasciculus; green: superior lateral fasciculus).

**Fig. 6: Diffusion Tensor Imaging (DTI) in AD**



MRI Alzheimer's biomarkers: Biomarkers are quantifiable medical signals (i.e., symptoms) [26]. Biomarkers have several definitions. Biomarkers are bodily parts, structures, or methods that may be analysed to identify the existence of a danger [27].

AD biomarkers have the following properties:

- 1) Capable of identifying basic characteristics of AD's neuropathology;
- 2) Capable of certifying neuropathologically confirmed AD cases;
- 3) Efficient, capable of identifying initial AD and capable of differentiating AD from different forms of dementias;
- 4) Reliable, non-invasive, easy to implement and inexpensive.

AD biomarkers include genetic, biochemical, and neuroimaging [28]. Due to their potential in AD detection, MRI biomarkers being studied. MRI may reveal atrophic alterations in the entorhinal cortex and hippocampus in early MCI, which may advance to the temporal and parietal lobes in AD and the frontal lobes in late AD. Functional MRI and DTI can detect Alzheimer's and non-damaged neurons. These two methodologies can analyse functional and structural link and provide biomarkers of Alzheimer's disease more power and resources, but they require regulation and authorisation to be therapeutically helpful. Structural MRI is the most effective and extensively utilised MRI biomarker for Alzheimer's disease, especially when hippocampus volume is involved.

## 2. LITERATURE SURVEY

Shi et al. [29] established a nonlinear learning strategy to improve AD and MCI biomarker identification (MCI). To make mapped data linearly separable for SVMs, the proposed approach learns a smooth nonlinear feature space transformation. Thin-plate spline (TPS) is the geometric model due to its malleability and ability to create smooth deformations. A deep network-based feature fusion approach is utilised to integrate cross-sectional and longitudinal MR brain image features. We show that the proposed feature transformation and fusion algorithms outperform state-of-the-art techniques on the ADNI dataset. Faturrahman et al. [30] suggested an AD classification algorithm based on structural modalities and Deep Belief Network (DBN). SVM was employed as an alternate classification model to DNN (DNN). Our technique beat SVM and other algorithms in a previous study. The DBN's accuracy, sensitivity, and specificity are all 0.9176. Ortiz et al. [31] discuss constructing longitudinal MRI models. This work provides an approach for modelling changes in Gray Matter (GM) across several brain areas during future testing. This will allow us to identify and link failing regions as a whole. This allows the discovery of differences between AD patients and controls. The longitudinal model incorporates GM volume and WM density. The obtained data showed that the strategy was efficient in extracting these patterns, which may be used to identify between Controls (CN) and AD individuals with 94% accuracy.

Nawaz et al. [32] propose using a Convolutional Neural Network to identify Alzheimer's by recreating the network's first layers from a previously trained AlexNet model (CNN). We classified deep features using SVM, KNN, and Random Forest (RF). According to the recommended scheme, a deep feature-based model has a higher accuracy rate (99.21%) than manual and deep learning procedures. The recommended strategy also outperforms best practises.

Wang et al. [33] built 3D-DenseNets to assist diagnose Alzheimer's and Parkinson's. Thicker links were built between succeeding layer nodes to improve data flow. Using a probability-based technique, 3D-DenseNets were blended with diverse designs. Extensive testing was done to assess the influence of 3D-hyper-parameters DenseNet's and topologies. The proposed model outscored rivals on ADNI.

Liang and Gu [34] introduced a WSL-based DL framework (ADGNET) for recognising and categorising AD with little annotations. The system has a backbone network, an attention mechanism, and a task network for image categorization and reconstruction. ADGNET performs well on 2D and 3D brain MRI data utilising only 20% of the labels for fine-tuning (Kappa, sensitivity, specificity, precision, accuracy, F1-score). The ADGNET's F1-score and sensitivity surpass two cutting-edge models. (Windows/CLR ResNext Simulator) Based on WSL, the recommended approach is a promising computer-assisted Alzheimer's diagnosis tool.



Using the ADNI (Alzheimer's disease neuroimaging initiative) experimental dataset, Sun et al. The proposed approach achieves 97.1% classification accuracy, 95.5% precision, 95.3% recall, and 95.4% F1 value at the macro level. The proposed model surpasses existing standards. Hon and Khan [36] developed a transfer learning approach in which VGG and Inception are pre-trained with weights from large benchmark datasets of natural pictures and the fully-connected layer is re-trained using a small sample of MRI images. Image entropy is utilised to pick training slices. Using the OASIS MRI dataset, we show that we can achieve state-of-the-art performance with 10x lower training volumes. Using fractal edge detection, Reju John et al. [37] diagnose Alzheimer's disease. Sobel and Prewitt filters improve edge detection efficiency and accuracy. They categorise MRI scans based on hippocampal mass, a measurement of grey and white matter. Fuzzy logic classifies changes in brain matter as Alzheimer's, the likelihood of Alzheimer's, or a healthy brain.

D.P. Devanand et al. [38] found that hippocampus, para hippocampal gyrus, and entorhinal cortex deformations predicted progression from mild cognitive impairment to Alzheimer's disease. Their technique expands earlier studies by analysing local brain surfaces. ANOVA, ANCOVA, and chi-square tests were used to compare AD converts, non-converters, and controls in terms of demographic and clinical variables and MRI scans. 134 people's hippocampal volumetric and surface morphometry are evaluated using the above methods. Andrea Chincarini et al. [39] used local MRI analysis to diagnose early and prodromal Alzheimer's disease. Analyzing hippocampal material does this. ADNI T1-weighted MRI data was segmented into slices and evaluated for features to identify regions of interest. Random Forest analysis was utilised to find key locations. After being filtered, these features were used to develop statistical models using Support Vector Machine, resulting in an AUC of 97% (sensitivity 89% at specificity 94%) for AD controls and 92% (sensitivity 89% at specificity 80%) for MCI converts. MCI converters may be discriminated from MCI non-converters with an AUC of 74% (sensitivity 72% and specificity 65%).

Elaheh Moradi et al. [40] employed machine learning to predict MCI patients' early MRI-based Alzheimer's conversion (LDS). This technique uses 1.5 T scanners to apply LDS on ANDI baseline T1-weighted MP-RAGE pictures. Using supervised and unstructured data, model parameters are refined. Unsupervised data helps the computer identify between Alzheimer's and Normal Cognition in brain MRI pictures. We use the LSD framework to the Random Forest framework to identify moderate cognitive impairment patients at high risk for Alzheimer's.

### 3. PROPOSED WORK

Listed below is the suggested research:

Deep learning is a kind of artificial intelligence in which a model learns to solve classification problems directly from a given dataset, such as photos, text, or speech. In

most cases, neural network architecture is employed to execute deep learning. As the number of network layers rises, the network's depth will increase. Deep neural networks may have several layers, as opposed to the two or three layers of normal neural networks. When it comes to artificial intelligence, identification applications like computer vision, facial recognition, natural language processing, audio recognition, social media filtering, and bioinformatics benefit greatly from deep learning approaches. It has performed as well as, and even better than, human specialists in several circumstances [41].

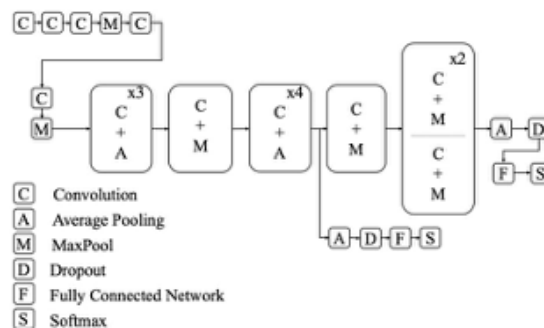
Deep learning is the most accurate machine learning technique compared to other approaches. The advances in the three technological areas have made this degree of accuracy possible.

- i. Access to vast volumes of labelled data was made simple and cost-free by the availability of big datasets.
- ii. Using powerful graphics processing units allows for a large amount of computational power. As a result, it will speed up the training of deep learning by minimising the amount of time spent on each data point.
- iii. Models of deep neural networks that have already been pre-trained. Pre-trained deep neural network models (such Alex Net, inception, VGG-16, and Resnet-50) may be retrained to carry out new classification and pattern recognition tasks with the use of the transfer learning approach [42].

### 3.1 Inception Architecture

For the proposed model, we recommend using the classification weights introduced in Inception V3 [43]. A neural network architecture for picture recognition, Inception V3 was trained on ImageNet to recognise a wide variety of real-world items. This trained model is used throughout the image-based learning process, and the weights are updated using the training data from this experiment to construct the three-group categorization of this research. Please indicate if the pictures are from AD, MCI, or CN. The Inception V3 model's internal structure is shown in Fig. 7.

**Fig. 7: Inception V3 Architecture**





A previous moniker for Inception was GoogleNet. Though it does decent work, VGG requires a lot of time and space to run. Inception cuts costs by constructing a bottleneck layer (1X1 convolutional filter). It uses convolutions of varying sizes, including 5X5, 3X3, and 1X1 convolutions, to pick up on finer distinctions. By swapping out the fully-connected layers that normally come after the final convolutional layer with global average pooling, the overall number of parameters is also reduced. InceptionV3's primary design goal is to "stretch" the network so it may process several kernel types simultaneously, hence addressing the problem of significant shifts in the location of features of interest across images. Multiple kernels may share the same level of operation thanks to the Inception modules. The original Inception proposal relied on this core idea (GoogLeNet). Auxiliary classifiers, representational bottlenecks, kernel factorization, and batch normalisation were all dealt with in subsequent iterations of the Inception architecture (InceptionV2 and InceptionV3). The 2015 ILSVRC image classification competition was won by the InceptionV3 framework.

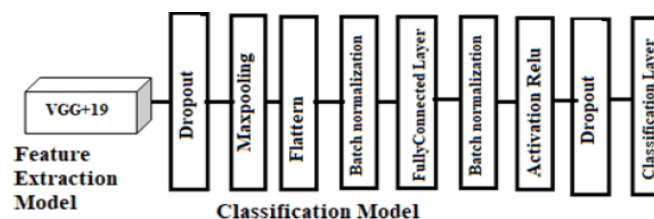
Network convolutional neural (CNN) designs that can provide the most ground-breaking improvements in image recognition are in great demand. The Inception architecture is illustrative of a system that achieves excellent performance at little computational cost. The researcher developed version 1.0 of the Inception deep network architecture. With the addition of batch normalisation to the original Inception idea, version 2 (Inception-v2) was born. The idea of factorization is then outlined, and the Inception-v3, Inception-v4, Inception ResNet V1, and Inception ResNet V2 designs are covered. The Inception model and the Inception ResNet model may be technically distinguished by the use of residual and non-residual versions of Inception. Therefore, the batch-normalization technique is performed just on top of the conventional layer, and not the residual summations, as a result of this differentiation.

### 3.2 Hybrid CNN Model

#### 3.2.1 Hybrid model

The VGG19 layer is utilised for feature extraction, while the additional CNN layers are used for classification in the hybrid model. With its 19 learning layers, the VGG19 is a deep learning model. It consists of a feature extraction layer and a classification layer. In this scenario, the layer responsible for classifying things is ignored. As seen in Fig 8, classification is finished by adding further layers.

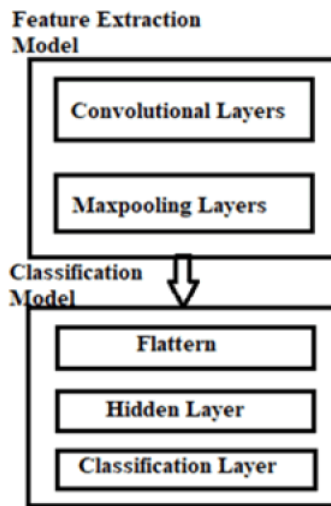
**Fig. 8: VGG19 and CNN**



### 3.2.2 CNN

The CNN model was utilised in both feature extraction and classification in Model 2. The structure of the model is shown in Fig 9.

**Fig 9: CNN model**



As shown in Fig 9, the feature extraction model is made up of 5 convolution layers, each of which is followed by a max-pooling layer. While the convolution layer is responsible for feature extraction, the pooling layer reduces the size of the input. When fed into the feature extraction model, an image with dimensions of 176 by 176 by three is transformed into an image with dimensions of 5 by 5 by 256. This is sent to the layer responsible for categorisation. There are four base layers, five connected thick layers, and a classification layer with four neurons for four classes.

### 3.2.3 Working architecture

The working flow of the entire system is depicted in Fig. 10.

**Fig. 10: The working flow of the entire CNN model**

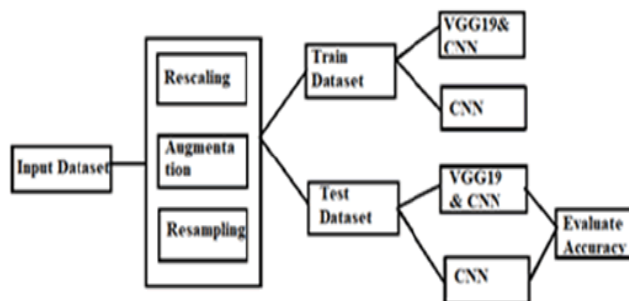


Figure 10 shows how the input dataset is pre-processed through rescaling, augmentation, and data resampling to boost the system's overall efficiency. Dataset pixels are rescaled from a range of 0 to 1 by dividing them by 255.0. Since we are using deep learning models, which need large training datasets, we first rescale the data and then enhance it. In order to avoid model overfitting, resampling is performed after augmentation. When the data has been cleaned and organised, it is split into a training set and a testing set. The model is "trained" using the train dataset, and "tested" using the test dataset. Two distinct datasets, train and validation, make up the whole train dataset. Use the validation dataset to improve the model's ability to generalise, or to find datasets that have never been seen before. Both models use the Rectified Linear Unit (ReLU) function in intermediate layers and the Softmax function in the classifier layer to accomplish multiple classifications. ReLU returns the same value as the input if the input is true and false otherwise. The biggest of the inputs is selected by the Softmax. The first equation is the ReLU equation, while the second represents the Softmax equation.

$$F(m) = n = \begin{cases} m, & \text{if } m > 0 \\ 0 & \text{otherwise} \end{cases} \quad (1)$$

(1) where  $m$  is an input and  $n$  is the output of ReLU.

$$\sigma(m)_t = \frac{e^{m_i}}{\sum_{j=1}^k e^{m_j}} \quad (2)$$

Where  $(m \rightarrow) i$  is vector input to the Softmax and  $e^{m_i}$  is exponential value of  $i$ th input.

#### 4. CONCLUSION AND DISCUSSION

In this research, a deep learning system for Alzheimer's disease forecasting was developed and implemented. It was also looked at how well the Inception v3 and Hybrid models performed. A hybrid deep learning model is superior to Inception V3 in predicting Alzheimer's illness.

#### REFERENCES

1. N. An, et al. Synergistic effects of APOE and CLU may increase the risk of Alzheimer's disease: Acceleration of atrophy in the volumes and shapes of the hippocampus and amygdala. *Journal of Alzheimers Disease*, 80 (3) (2021), pp. 1311-1327, 10.3233/jad-201162.
2. J. Contador, et al. Longitudinal brain atrophy and CSF biomarkers in early-onset Alzheimer's disease *NeuroImage. Clinical*, 32 (2021), Article 102804, 10.1016/j.nicl.2021.102804.
3. K. Kamagata, et al. Diagnostic imaging of dementia with Lewy bodies by susceptibility-weighted imaging of nigrosomes versus striatal dopamine transporter single-photon emission computed tomography: A retrospective observational study. *Neuroradiology*, 59 (1) (2017), pp. 89-98, 10.1007/s00234-016-1773-z.
4. F. Falahati, E. Westman, A. Simmons, Multivariate data analysis and machine learning in Alzheimer's disease with a focus on structural magnetic resonance imaging *Journal of Alzheimers Disease*, 41 (3) (2014), pp. 685-708, 10.3233/jad-131928

5. W.E. Klunk, et al. Imaging brain amyloid in Alzheimer's disease with Pittsburgh compound-B *Annals of Neurology*, 55 (3) (2004), pp. 306-319, 10.1002/ana.20009.
6. H.J. Rosen, J.H. Kramer, M.L. Gorno-Tempini, N. Schuff, M. Weiner, B.L. Miller, Patterns of cerebral atrophy in primary progressive aphasia, *The American Journal of Geriatric Psychiatry: Official Journal of the American Association for Geriatric Psychiatry*, 10 (1) (2002), pp. 89-97, 10.1176/appi.ajgp.10.1.89.
7. R. De Flores, R. La Joie, G. Chetelat, Structural imaging of hippocampal subfields in healthy aging and Alzheimer's disease. *Neuroscience*, 309 (2015), pp. 29-50, 10.1016/j.neuroscience.2015.08.033.
8. C. Testa, et al. Comparison between the accuracy of voxel-based morphometry and hippocampal volumetry in Alzheimer's disease, *Journal of Magnetic Resonance Imaging*, 19 (3) (2004), pp. 274-282, 10.1002/jmri.20001.
9. H. Nguyen, N.N. Chu, An introduction to deep learning research for Alzheimer's disease, *IEEE Consumer Electronics Magazine*, 10 (3) (2020), pp. 72-75.
10. D. Prakash, N. Madusanka, S. Bhattacharjee, C.H. Kim, H.G. Park, H.K. Choi Diagnosing Alzheimer's Disease based on Multiclass MRI Scans using Transfer Learning Techniques, *Current medical imaging* (2021), 10.2174/1573405617666210127161812.
11. N. L. Hill and J. Mogle, "Alzheimer's disease risk factors as mediators of subjective memory impairment and objective memory decline: Protocol for a construct-level replication analysis," *BMC Geriatrics*, vol. 18, no. 1, Dec. 2018.
12. D. D. Nolte, J. J. Turek, and K. Jeong, "Method and apparatus for motility contrast imaging," U.S. 20 150 062 592 A1, Oct. 16, 2018.
13. S. J. Makaretz, M. Quimby, J. Collins, N. Makris, S. McGinnis, A. Schultz, N. Vasdev, K. A. Johnson, and B. C. Dickerson, "Flortaucipir tau PET imaging in semantic variant primary progressive aphasia," *J. Neurol., Neurosurg. Psychiatry*, vol. 89, no. 10, pp. 1024–1031, Oct. 2018.
14. M. Waser, T. Benke, P. Dal-Bianco, H. Garn, J. A. Mosbacher, G. Ransmayr, R. Schmidt, S. Seiler, H. B. D. Sorensen, and P. J. Jennum, "Neuroimaging markers of global cognition in early Alzheimer's disease: A magnetic resonance imaging-electroencephalography study," *Brain Behav.*, vol. 9, no. 1, Jan. 2019, Art. no. e01197.
15. K. Trojchanec, I. Kitanovski, I. Dimitrovski, and S. Loshkovska, "Longitudinal brain MRI retrieval for Alzheimer's disease using different temporal information," *IEEE Access*, vol. 6, pp. 9703–9712, 2018.
16. M. Sagnou, B. Mavroidi, A. Shegani, M. Paravatou-Petsotas, C. Raptopoulou, V. Psycharis, I. Pirmettis, M. S. Papadopoulos, and M. Pelecanou, "Remarkable brain penetration of cyclopentadienyl M(CO)<sub>3</sub> (M = <sup>99m</sup>Tc, Re) derivatives of benzothiazole and benzimidazole paves the way for their application as diagnostic, with single-photon-emission computed tomography (spect), and therapeutic agents for Alzheimer's disease," *J. Med. Chem.*, vol. 62, no. 5, pp. 2638–2650, 2019.
17. Begcevic, D. Brinc, M. Brown, E. Martinez-Morillo, O. Goldhardt, T. Grimmer, V. Magdolen, I. Batruch, and E. P. Diamandis, "Brain-related proteins as potential CSF biomarkers of Alzheimer's disease: A targeted mass spectrometry approach," *J. Proteomics*, vol. 182, pp. 12–20, Jun. 2018.
18. N. A. Johnson, G.-H. Jahng, M. W. Weiner, B. L. Miller, H. C. Chui, W. J. Jagust, M. L. Gorno-

- Tempini, and N. Schuff, "Pattern of cerebral hypoperfusion in Alzheimer disease and mild cognitive impairment measured with arterial spin-labeling MR imaging: Initial experience," *Radiology*, vol. 234, no. 3, pp. 851–859, Mar. 2005.
19. Y. Li, S. Dolui, D.-F. Xie, and Z. Wang, "Priors-guided slice-wise adaptive outlier cleaning for arterial spin labeling perfusion MRI," *J. Neurosci. Methods*, vol. 307, pp. 248–253, Sep. 2018.
  20. Drzezga, D. Altomare, C. Festari, J. Arbizu, S. Orini, K. Herholz, P. Nestor, F. Agosta, F. Bouwman, F. Nobili, Z. Walker, G. B. Frisoni, and M. Boccardi, "Diagnostic utility of 18F-fluorodeoxyglucose positron emission tomography (FDG-PET) in asymptomatic subjects at increased risk for Alzheimer's disease," *Eur. J. Nucl. Med. Mol. Imag.*, vol. 45, no. 9, pp. 1487–1496, 2018.
  21. V. L. Villemagne, V. Doré, S. C. Burnham, C. L. Masters, and C. C. Rowe, "Imaging tau and amyloid- $\beta$  proteinopathies in Alzheimer disease and other conditions," *Nature Rev. Neurol.*, vol. 14, no. 4, pp. 225–236, Apr. 2018.
  22. R. Ducksbury, T. Whitfield, and Z. Walker, "SPECT/PET findings in Lewy body dementia," in *PET and SPECT in Neurology*. Berlin, Germany: Springer, 2014, pp. 373–415.
  23. D. A. Wolk, Z. Zhang, S. Boudhar, C. M. Clark, M. J. Pontecorvo, and S. E. Arnold, "Amyloid imaging in Alzheimer's disease: Comparison of florbetapir and pittsburgh compound-B positron emission tomography," *J. Neurol., Neurosurg. Psychiatry*, vol. 83, no. 9, pp. 923–926, Sep. 2012.
  24. M. J. Knight, A. Wearn, E. Coulthard, and R. A. Kauppinen, "T2 relaxometry and diffusion tensor indices of the hippocampus and entorhinal cortex improve sensitivity and specificity of MRI to detect amnesic mild cognitive impairment and Alzheimer's disease dementia," *J. Magn. Reson. Imag.*, vol. 49, no. 2, pp. 445–455, Feb. 2019.
  25. Kumar, S. Singh, A. Chaurasiya, and A. Singh, "Implication of preclinical biomarkers in identification of mild cognitive impairment (MCI) and Alzheimer's disease: Promises and future challenges," *Res. Rep.*, vol. 2, pp. 1–16, May 2018.
  26. L. Mosconi, M. Walters, J. Sterling, C. Quinn, P. McHugh, R. E. Andrews, D. C. Matthews, C. Ganzer, R. S. Osorio, R. S. Isaacson, M. J. De Leon, and A. Convit, "Lifestyle and vascular risk effects on MRI-based biomarkers of Alzheimer's disease: A cross-sectional study of middleaged adults from the broader New York city area," *BMJ Open*, vol. 8, no. 3, Mar. 2018, Art. no. e019362.
  27. M. Mussap, A. Noto, F. Cibecchini, and V. Fanos, "The importance of biomarkers in neonatology," *Seminars Fetal Neonatal Med.*, vol. 18, no. 1, pp. 56–64, Feb. 2013.
  28. Cedazo-Minguez and B. Winblad, "Biomarkers for Alzheimer's disease and other forms of dementia: Clinical needs, limitations and future aspects," *Exp. Gerontol.*, vol. 45, no. 1, pp. 5–14, Jan. 2010.
  29. Shi, Y. Chen, P. Zhang, C.D. Smith, J. Liu, I. Alzheimers Dis Neuroimaging, Nonlinear feature transformation and deep fusion for Alzheimer's Disease staging analysis, *Pattern Recognition*, 63 (2017), pp. 487-498, 10.1016/j.patcog.2016.09.032.
  30. M. Faturrahman, I. Wasito, N. Hanifah, R. Mufidah, Structural MRI classification for Alzheimer's disease detection using deep belief network, *Proceedings of the 11th international conference on information & communication technology and system (ICTS) (2017)*, pp. 37-42, 10.1109/ICTS.2017.8265643.
  31. Ortiz, J. Munilla, F.J. Martínez-Murcia, J.M. Górriz, J. Ramírez, A.S.D.N. Initiative, Learning

longitudinal MRI patterns by SICE and deep learning: Assessing the Alzheimer's disease progression, Proceedings of the Annual conference on medical image understanding and analysis, Springer (2017), pp. 413-424.

32. H. Nawaz, M. Maqsood, S. Afzal, F. Aadil, I. Mehmood, S. Rho, A deep feature-based real-time system for Alzheimer disease stage detection, *Multimedia Tools and Applications* (2020), 10.1007/s11042-020-09087-y.
33. H. Wang, et al. Ensemble of 3D densely connected convolutional network for diagnosis of mild cognitive impairment and Alzheimer's disease, *Neurocomputing*, 333 (2019), pp. 145-156, 10.1016/j.neucom.2018.12.018.
34. S. Liang, Y. Gu Computer-aided diagnosis of Alzheimer's disease through weak supervision deep learning framework with attention mechanism, *Sensors*, 21 (1) (2021), p. 220.
35. M. Hon, N.M. Khan, Towards Alzheimer's disease classification through transfer learning, *Proceedings of the IEEE international conference on bioinformatics and biomedicine (BIBM)*, IEEE (2017), pp. 1166-1169.
36. H. Sun, A. Wang, W. Wang, C. Liu, An improved deep residual network prediction model for the early diagnosis of Alzheimer's disease, *Sensors*, 21 (12) (2021), p. 4182, 10.3390/s21124182.
37. John R et al. (2018). Detection of Alzheimers Disease Using Fractional Edge Detection. *Global J Technol Optim* 9: 230. doi:10.4172/2229-8711.1000230
38. D.P. Devanand et al. (2012). MRI hippocampal and entorhinal cortex mapping in predicting conversion to Alzheimer's disease. *NeuroImage* 60 (2012) 16221629.
39. Andrea Chincarini et al. (2011). Local MRI analysis approach in the diagnosis of early and prodromal Alzheimer's disease. *NeuroImage* 58 (2011) 469480.
40. Elaheh Moradi et al. (2015). Machine learning framework for early MRI-based Alzheimer's conversion prediction in MCI subjects. *NeuroImage* 104 (2015) 398412.
41. Ian Goodfellow, Yoshua Bengio, et al., 2016 Deep learning e-book (MIT press).
42. Geoffrey E Hinton 2011 Machine learning for neuroscience *Neural Systems & Circuits* 12(2011) pp 1-12.
43. Christian Szegedy et al. (2015). Rethinking the Inception Architecture for Computer Vision. *ArXiv: 1512.00567v3 [cs.CV]* 11 Dec 2015.